Journal of Applied Polymer Science

Modification of Disposable Screen-Printed Carbon Electrode Surfaces with Conductive Electrospun Nanofibers for Biosensor Applications

Pongpol Ekabutr,[1] Orawan Chailapakul,[2,3] Pitt Supaphol[1,3]

[1]The Petroleum and Petrochemical College, Chulalongkorn University, Thailand

[2]Electrochemistry and Optical Spectroscopy Research Unit, Department of Chemistry, Faculty of Science, Chulalongkorn University, Thailand

[3]Center of Excellence on Petrochemical and Materials Technology (PETROMAT), Chulalongkorn University, Patumwan, Bangkok 10330, Thailand

Correspondence to: Pitt Supaphol (E - mail: pitt.s@chula.ac.th)

ABSTRACT: In this work, we describe an alternative approach to the surface modification of screen-printed carbon electrodes (SPCEs) to fabricate a polypyrrole/polyacrylonitrile multiwall carbon nanotube-modified screen-printed carbon electrode (PPy/PAN-MWCNT/SPCE) using a two-step process. First, PAN loaded with 5 wt % of MWCNTs was electrospun onto a carbon layer. The CNT-embedded PAN electrospun nanofibers (average diameter $\approx$ 200 nm) were subsequently coated with a PPy layer via vapor-phase polymerization using *p*-toluenesulfonate as an oxidizing agent in a vacuum system. The electrochemical behavior of both the unmodified and the modified SPCEs were compared using cyclic voltammetry (CV) with common electroactive analytes in order to optimize the electrospinning and the vapor-phase parameters. By incorporating glucose oxidase(GOX) as an enzymatic model into the modified electrode without a mediator, we conducted a calibration study which showed that glucose could be detected by an amperometer over a linear range of 0.25–6 m*M* with a LOD of 15.51 μM and a sensitivity of 5.41 μA/m*M* cm^2. With a mediator, the glucose detection can be performed at low potential over a linear range of 0.125–7 m*M* with a LOD of 0.98 m*M* and a sensitivity of 14.62 μA/m*M* cm^2. Therefore, the novel modified electrode is a promising new device for biosensor applications. © 2013 Wiley Periodicals, Inc. J. Appl. Polym. Sci. 130: 3885–3893, 2013

KEYWORDS: sensors and actuators; conducting polymers; fibers; nanostructured polymers; composites

Received 30 March 2013; accepted 8 June 2013; Published online 2 July 2013

DOI: 10.1002/app.39651

INTRODUCTION

In recent years, a vast number of reports on screen-printing carbon electrode (SPCE) technology have been used to develop biosensors that detect biological molecules in applications, such as environmental,[1] biomedical,[2] microbiological,[3] healthcare,[4] and chemical/biochemical analyses.[5] Because an SPCE is inexpensive and can be used as a disposable electrode with large-scale production capability, a number of methods have been devised to increase the surface area of SPCEs to enhance their sensitivity for electrochemical detection. For example, this enhanced sensitivity can be achieved by coating an SPCE with a conductive polymer, such as polypyrrole (PPy),[6] polyaniline (PANI),[7] or poly(3,4-ethylenedioxythiophene):poly(styrene-sulfonate) acid (PEDOT:PSS),[8] via an electropolymerization process using a potentiodynamic, potentiostatic, or galvanostatic mode. These processes can be used in combination with chemical/biological components that are embedded in the SPCE structures. In amperometric biosensors, enzyme electrodes that contain oxidase enzymes can catalyze substrates, such as glucose,[9] uric acid,[10] or lactate,[2] by reducing oxygen to form hydrogen peroxide (H_2O_2), and the oxidation current can be evaluated.[11]

Among the different techniques that are used to obtain nanostructured surfaces, electrospinning techniques produce nanofibers with a large surface area that is one to two orders of magnitude larger than those found in continuous films. Electrospun fiber matrices also exhibit a high porosity and the individual fibers provide good features for the incorporation of active composites, such as metal nanoparticles,[12] graphene,[13] or carbon nanotubes (CNTs),[14] to improve the electron-transfer activities. CNTs are extensively used in biosensors because of their unique tubular structure with a nanoscale diameter, high conductivity, and outstanding mechanical properties.[15]

Vapor-phase polymerization (VPP) has been used to synthesize and to optimize intrinsically conducting polymers (ICPs). The substrates were coated with oxidizing agents, such as $FeCl_3$,[16]

Fe(III) *p*-toluenesulfonate (FeTos),[17] benzenesulfonic acid, *p*-dodecylbenzenesulfonic acid (DBSA), and *p*-ethylbenzenesulfonic acid,[18] using simple coating methods. Then, the oxidant-coated substrates were exposed to ICP monomers. When monomer molecules evaporated from the oxidant-coated locations, they were rapidly polymerized to form a conductive thin film on the substrate surface. The advantages of this technique are that it can be performed on various substrates including insulator in specific area and VPP is one of the self-assembling polymerization techniques performing under gas-phase and can easily produce pure conducting polymer films with excellent electronic conductivity properties.[19] In this work, VPP was used to coat a PPy layer onto electrospun nanofibers.

The aim of this study is to modify an SCPE surface through the preparation of a PPy/PAN-MWCNT/SPCE electrode with a PPy coating on CNT-embedded PAN electrospun nanofibers, which is key in the enhancement of the electrode electrochemical performance. First, the redox behaviors of the unmodified/modified electrode were studied in a ferri/ferrocyanide solution to optimize the electrode surface modification. Second, the H_2O_2 detection of the modified electrode and any interference were studied. Glucose detection was also studied; glucose oxidase was used as a representative enzyme without and with the addition of a mediator. The performance of PPy/PAN-MWCNT/SPCE electrodes with respect to their sensitivity, detection limits, and calibration curves are described and discussed.

EXPERIMENTAL DETAILS

Materials

All of the chemicals used in this research were analytical grade. D-(+)-Glucose, glucose oxidase (GOX, EC 1.1.3.4, *Aspergillus niger*, 10,000 units), *N*,*N*-dimethylformamide (DMF), 98% pyrrole monomer, Fe(III) *p*-toluenesulfonate (FeTos), 1-butanol, and pyridine were purchased from Sigma-Aldrich. Polyacrylonitrile (PAN) microfibers in which the polymer (Mw ~55.5 kDa) contained 91.4 wt % acrylonitrile monomer (CH_2=CHCN) and 8.6 wt % methylacrylate comonomer (CH_2=CHCOOHCH$_3$), were used as raw material in the electrospinning process and were received from Thai Acrylic Fiber (Thailand). Multiwall carbon nanotubes (MWCNTs, 10–20 nm) were purchased from Chengdu Alpha Nano Technology (China). A phosphate buffer solution (pH 3–9, adjusted using 1.0 *M* HCl and 1.0 *M* NaOH solutions) was prepared using dihydrogen phosphate (Fluka, Switzerland). Carbon ink (C2070424D2) was purchased from the Gwent group (Torfaen, UK). Silver chloride ink (Electrodag 7019) was obtained from the Acheson Colloids. All chemicals were used as received without further purification. The electrospinning apparatus was a Gamma High Voltage Research D-ES30PN/M692 equipped with a dc power source.

Electrochemical measurements were performed using a potentiostat (CHI 1207A, CH Instruments) at room temperature (25 ± 1°C). Cyclic voltammetry measurements were performed using a conventional three-electrode system, which consisted of a modified/unmodified SPCE as the working electrode with a working area of 0.50 cm^2, an Ag/AgCl electrode as the reference electrode, and platinum wire as the counter electrode.

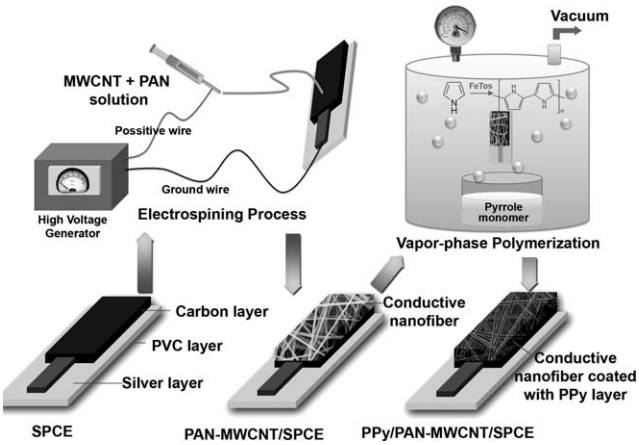

Figure 1. Schematic of electrode fabrication.

Screen-Printed Electrode Fabrication

SPCEs were fabricated on a PVC plastic sheet(10 × 35 mm^2). First, silver ink was spread over the PVC surface twice using a manual screen printing technique. Next, carbon layer (10 × 20 mm^2) was also coated two times on top of the silver layer (3 × 15 mm^2). In each spreading, the SPCE was put in an oven at 60°C for 60 min to get rid of any solvent. Further surface modifications of the SPCE surfaces were performed using the electrospinning and vapor-phase polymerization (VPP) techniques, as shown in Figure 1. The unmodified SPCE was labeled as SPCE.

Electrospinning Process

The SPCE surfaces were modified with conductive PAN-based nanofibers by electrospinning a 10 wt % PAN solution in DMF in which MWCNTs at a fixed concentration of were dispersed in the PAN solution and sonicated for 30 min with a homogenizer. Figure 1 shows the experimental apparatus that was used for the electrospinning process. A 20 mL syringe with a capillary tip (D = 0.5 mm^2) was placed and clamped near an anode connected to a high-voltage power supply. The cathode was connected to the silver layer with a 15 kV applied voltage. The distance between the electrode and the nozzle was 15 cm, and various electrospinning times (1–30 min) were used at room temperature (25 ± 1°C).

Vapor-Phase Polymerization (VPP) of the PPy Layer

After the electrospinning process, the VPP of the PPy layer was conducted in the vacuum chamber setup (Figure 1). The PAN–MWCNT/SPCEs were first coated with FeTos at various concentrations (20–60% w/v) in *n*-butanol and pyridine. The oxidant-coated electrodes were subsequently heated on a hot plate at 60°C for 3 min until the solvent evaporated. The electrodes were then exposed to pyrrole vapor in a sealed vacuum chamber. After polymerization, the electrodes were heated at 60°C for 1 hour to ensure complete evaporation of the pyrrole monomer. The electrodes were then washed with absolute ethanol for 5 min, followed by rinsing with deionized water for 5 min. Finally, the electrodes were dried under vacuum at room temperature for 2 hours. The completely PPy-coated electrodes were labeled PPy/PAN–MWCNT/SPCE.

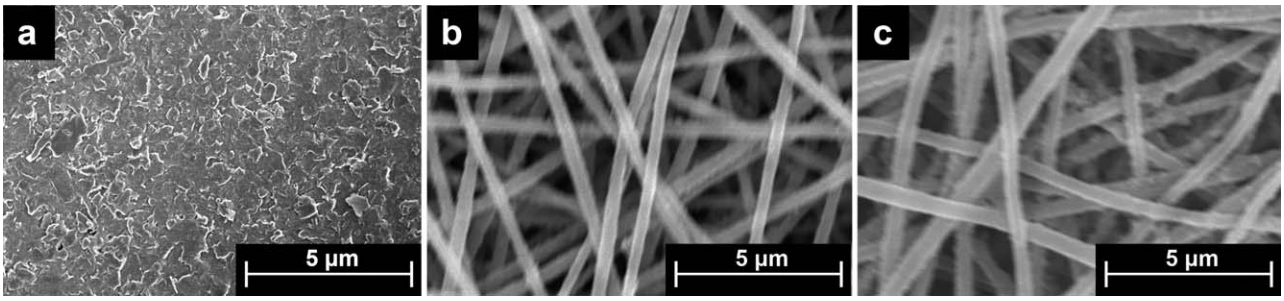

Figure 2. SEM images of the surface morphologies of the (a) SPCE, (b) PAN–MWCNT/SPCE, and (c) PPy/PAN–MWCNT/SPCE.

Electrochemical Studies of the PPy/PAN–MWCNT/SPCE in a Ferri/Ferro Solution

The electrochemical behavior of the modified/unmodified electrodes was studied using cyclic voltammetry (CV). Cyclic voltammograms were obtained at scan rates of 10–500 mV/s using 5 m*M* $Fe(CN)_6^{3-/4-}$ in 0.1 *M* PBS at a pH of 7.4. To study the anodic current responses of the electrodes, the scan rate was fixed at 50 mV/s in 0.1 *M* PBS at a pH of 7.4. The background current was subtracted from the oxidative current to obtain the anodic current values from the CV results.

Cyclic Voltammetry Measurements of Hydrogen Peroxide at the Electrodes

The cyclic voltammograms of the electrodes were evaluated by scanning from 0 to +1.6 V at a scan rate of 50 mV/s using a 2 mL aliquot of 10 m*M* H_2O_2 in 0.1 *M* PBS at a pH of 7.4. The CV of the background of each electrode is illustrated in Figure 6(a).

Amperometric Response to Hydrogen Peroxide Using the Modified Electrodes

The potential response of the anodic current peak of the SPCE and the PPy/PAN–MWCNT/SPCE for the detection of the H_2O_2 oxidation current is +1.4 and +1.2 V, respectively, with respect to an Ag/AgCl electrode. These potential responses were used to construct the plots of anodic current versus time, as shown in Figure 6(b). Initially, the background current was measured until the current became constant. Then, a concentration series of H_2O_2 was added to the solution, which resulted in an immediate increase in the anodic current until it reached a steady-state when approaching the 50 second mark. Finally, the differences between these anodic current values were studied. The effects of the pH, the concentrations of the supporting electrolyte, and the calibration for H_2O_2 detection were also studied.

Electrochemical Impedance Spectroscopy Studies

For the electrochemical impedance spectroscopy (EIS) were carried out by using Autolab PGSTAT30 (Eco Chemie, B.V., The Netherlands). The impedance spectra of electrodes were performed in the same 5 m*M* $Fe(CN)_6^{3-/4-}$ in 0.1 *M* PBS with a pH of 7.4. The frequency range of EIS measurements was 0.01–100 kHz, at 100 measuring points and using a sinusoidal waveform of 10 mV at the potential of the +0.5 V vs. saturated Ag/AgCl. All experiments were recorded in triplicate.

Enzyme Electrode Preparation

The dropping method was used for enzyme electrode preparation. The procedures were as follows: various concentrations of GOX solutions (0.1–1.0 g/mL) were prepared in 0.1 *M* PBS at a pH of 7.4 in vials. Afterward, 20 μL of the prepared enzyme solutions were dropped onto the PPy/PAN-MWCNT/SPCE surface, followed by 1 hour of air drying. The samples were maintained at 4°C until use. For the significance of mediated system, 5 m*M* of $K_3[Fe(CN)_6]$ was used as mediator. The tests were carried out the same method as amperometry and CV of H_2O_2 studies.

Calibration Studies Using Amperometry with the Modified Electrode for Glucose Detection

Calibration studies were conducted on the PPy/PAN–MWCNT/SPCE with 0.1 g/mL of GOX as the enzyme model. The glucose that was used as the substrate was prepared in various concentrations that ranged from 0.125 to 20 m*M* in 0.1 *M* PBS with a pH of 7.4. For the amperometric measurements with/without mediator, the potential was fixed at +0.36 V and +1.2 V, respectively, which was the characteristic response of the PPy/PAN–MWCNT/SPCE to glucose. The data were monitored over the range of 0–50 s. The glucose additions were made without the solution in the cell being stirred. The limit of detection (LOD, 3 S/N) was estimated for the PPy/PAN–MWCNT/SPCE.

Surface Morphology Studies

The morphologies of both the modified and unmodified electrodes were observed using a Hitachi S-4800 field-emission scanning electron microscope (FE-SEM) operated at 10 kV; the SemAphore 4.0 software was used for image processing. Each electrode was coated with a thin platinum layer using a platinum sputtering device before SEM observation.

RESULTS AND DISCUSSION

Morphological Analysis

Figure 2(a–c) shows the SEM images of the SPCE, the PAN–MWCNT/SPCE, and the PPy/PAN–MWCNT/SPCE. The SPCE exhibits a rough surface with a large grain size of several microns because of the solvent evaporation from the carbon ink. For the PAN–MWCNT/SPCE, PAN loaded with 5 wt % MWCNTs was electrospun on top of the carbon layer, as described in Figure 1. As evident from the SEM images, a longer electrospinning time resulted in more random-like conductive nanofibers covering the electrode surface. The 5 wt %

Applied Polymer SCIENCE

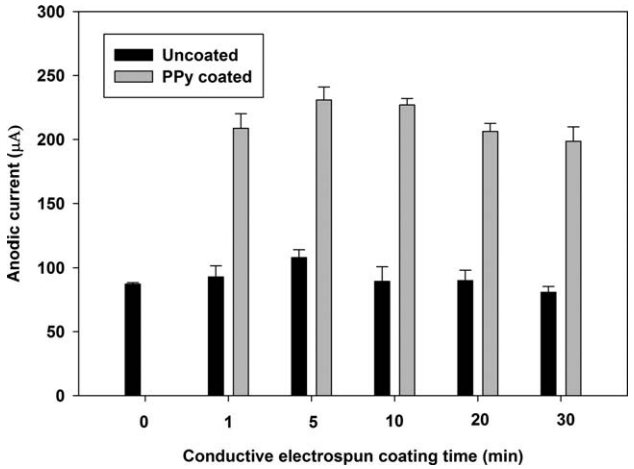

Figure 3. Anodic current response of the modified electrodes before and after the PPy layer was coated using 5 m*M* $Fe(CN)_6^{3-/4-}$ in 0.1 *M* PBS with a pH of 7.4 as a function of the electrospinning time.

MWCNTs in the conductive fibers were well dispersed, which led to a perfectly smooth and contoured fiber; however, an excessively high MWCNT loading can cause bead-structured fibers due to MWCNT agglomeration.[20] The average conductive fiber diameter of the PAN–MWCNT/SPCE was ~308 ± 48 nm, and the surface area was large.[14]

For the final modification step, the conductive electrospun layer was coated with PPy via VPP in a vacuum chamber. The pyrrole monomer evaporated rapidly and then polymerized into PPy on the fiber surface, which resulted in a drastically increased fiber diameter of 420–590 nm within the first minute of exposure; it also resulted in a color change from uncoated white fibers to black. Figure 4(a) shows the thickness of the PPy film covering the electrospun fibers, which increased in proportion to the polymerization time. However, the thickness and morphology of the coated fibers depended on the concentration of the oxidizing agent. When the oxidizing agent concentration was increased, the PPy film formation also increased. Moreover, in a high FeTos concentration (60% w/v), the viscosity of the coating was also high, and PPy polymerized as a thick film that covered the electrode and caused a film-like polymer coating on the electrode surface.[21]

Electrochemical Behavior of the Fabricated Electrodes

The electrochemical behavior of the fabricated electrodes was studied by cyclic voltammetry using 5 m*M* $Fe(CN)_6^{3-/4-}$ as a reversible redox couple model.[22] The redox peaks (oxidation/reduction) and voltage windows were recorded in the range of −0.6 to +1.0 V. The cathodic and anodic current responses were observed for the SPCE (+0.55 V/−0.2 V), PAN–MWCNT/SPCE (+0.4 V/−0.1 V) and PPy/PAN–MWCNT/SPCE (+0.3 V/+0.15 V). The observations were interesting. The electrochemical efficacy of the electrodes was evaluated using the CV responses, and the modified and unmodified electrode surfaces were compared. Figure 5(a) shows that the CV of each electrode exhibited the reversible redox peaks of $Fe(CN)_6^{3-/4-}$ with an increased oxidation/reduction current (233 ± 6 and 231 ± 2 μA for the PPy/PAN–MWCNT/SPCE, 70.9 ± 3 and 69.3 ± 2 μA for the PAN–MWCNT/SPCE, and 25.1 ± 1 and 23.2 ± 2 μA for the SPCE). Moreover, the presence of the conductive nanofibrous structure and the presence of the PPy layer on the electrode surfaces resulted in a decrease in the separation between E_{pa} and E_{pc}, ΔE_p, and an increase in the electrochemical sensitivity.[23]

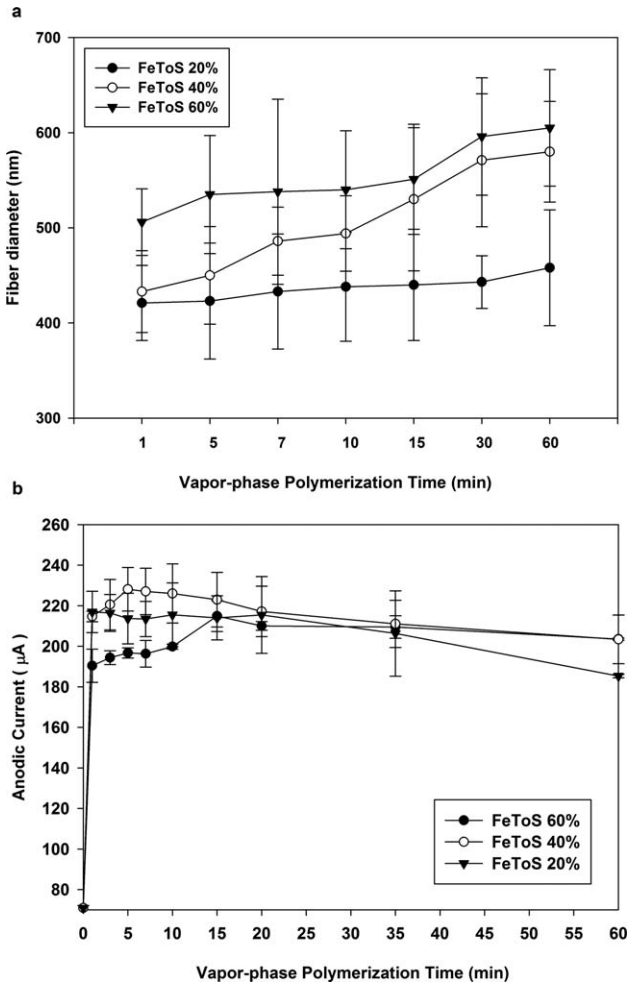

Figure 4. (a) The effect of the FeTos oxidant concentration on the fiber diameter, and (b) effect of the FeTos oxidant concentration on the anodic current response using 5 m*M* $Fe(CN)_6^{3-/4-}$ in 0.1 *M* PBS with a pH of 7.4.

The electron transfer on the electrode surface can be improved through the use of the electrospinning technique with conductive nanofibers.[24,25] From the CV, the SPCE covered with conductive nanofibers and coated with a PPy layer (the PPy/PAN–MWCNT/SPCE) exhibited the greatest oxidation peak amplitudes, ~4.5 and 2.5 times greater than those of the SPCE and the PAN–MWCNT/SPCE, respectively. The effects of the conductive nanofiber coating on the SPCE surface and the effects of the VPP of PPy were also studied in terms of the anodic current for each set of conditions. Figure 3 shows the anodic current responses of the PAN–MWCNT/SPCE before (black bars) and after (grey bars) the nanofibers were coated with the PPy layer. A difference is evident at the 5 min coating mark, which is the best coating time for the fabrication of the PAN–MWCNT/SPCE because a longer coating time can create a

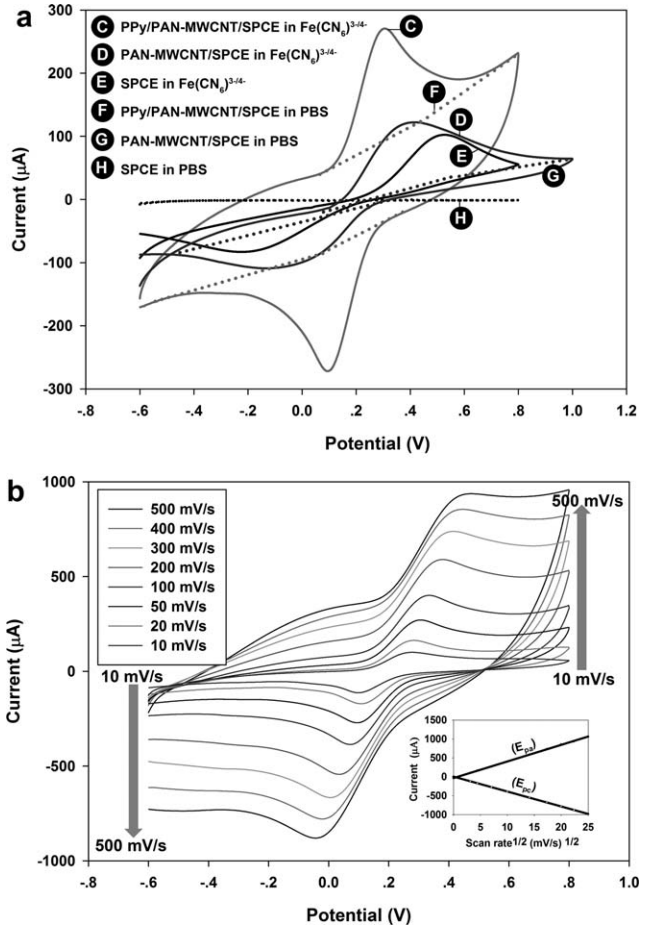

Figure 5. (a) Cyclic voltammograms of different modified electrodes measured using 5 m*M* $Fe(CN)_6^{3-/4-}$ in 0.1 *M* PBS with a pH of 7.4 at a scan rate of 50 mV/s. (b) Cyclic voltammograms of the PPy/PAN-MWCNT/SPCE electrode at different scan rates; (inset) plot of the linear relation of the current vs. the scan rate$^{1/2}$.

current barrier on the electrode surface.[26] Nevertheless, only the PAN electrospun nanofibers without MWCNTs on the SPCE surface (the result not shown in this article exhibited a drastic increase in ΔE_p: +0.6 V for oxidation (E_{pa}) and −0.3 V for reduction (E_{pc}). The enhancement of the anodic current through coating the nanofibers with the PPy layer produced the same trend. In the case of VPP, Figure 4(b) shows that the use of high concentrations of an oxidizing agent to obtain a thick PPy layer was not a suitable method for obtaining excellent electrode surface electrochemical activity.[27] In this experiment, the best conditions for obtaining the highest anodic current were 40% (w/v) FeTos and 5 min of polymerization. Therefore, these conditions were used to modify the PPy/PAN–MWCNT/SPCE.

In addition, the effect of the CV scan rate on the performance of the electrodes was studied, and the results are shown in Figure 5(a), which shows the characteristic cyclic voltammograms of the PPy/PAN–MWCNT/SPCE in 0.1 *M* PBS with a pH of 7.4 at different scan rates. When the scan rate was increased from 10 to 500 mVs^{-1}, the oxidation peak potential gradually shifted to a positive potential. The oxidation peak current, I_p, and the reduction peak, I_c, are governed by the Randle–Sevcik relation, shown in eq. (1):

$$I_p = kn^{3/2}AD^{1/2}C^b\upsilon^{1/2} \quad (1)$$

where the constant k is equal to 2.72×10^5, n is the number of moles of electrons that are transferred per mole of electroactive species (ferricyanide), A is the electrode area in cm^2, D is the diffusion coefficient in cm^2/s, C^b is the solution concentration in mol/L, and υ is the potential scan rate in V/s. The I_p is linearly proportional to the bulk concentration of the electroactive species, C^b, and to the square root of the scan rate, $\upsilon^{1/2}$. Therefore, an interesting diagnostic is a plot of I_p vs. $\upsilon^{1/2}$, as shown in Figure 5(b); both the oxidation peak current (I_a) and the reduction peak current (I_c) of the PPy/PAN–MWCNT/SPCE exhibited linear responses. The electrode reaction can be reasonably deduced as being controlled by a radial diffusion process[2], which is related to the mass transport rate of the electroactive species to the electrode surface.[28] Moreover, the incorporation of both conductive nanofibers and a PPy layer on the electrode surface makes the PPy/PAN–MWCNT/SPCE system quasi-reversible ($I_c/I_a \neq 1$).[23]

EIS is a very important tool for interface properties of electrodes. Figure 10 displayed Nyquist plots of SPCE, PAN-MWCNT/SPCE and PPy/PAN-MWCNT/SPCE at +0.4 V. The semicircle part corresponds to the electron-transfer controlled process that the diameter represents the magnitude of charge-transfer resistance at the electrode surface. The highest semicircle of SPCE suggested a high value of charge-transfer resistance, whereas the modified electrodes were much smaller than that of SPCE. The charge-transfer resistance of the PPy/PAN-MWCNT/SPCE exhibited the lowest among the three electrodes. This is due to PPy forms a charge-transfer complex and high surface area with a nanofibrous structure fabricated by electrospining and VPP.[14] In addition, the reports of SPCE modified with polypyrrole film can provide greatly enhanced electrochemical reactivity compared to conventional SPCE, which confirmed the results in this research [29,30]

Performance of the Modified Electrodes in a Hydrogen Peroxide Standard Solution

A CV study was used to determine whether H_2O_2 could be measured using the proposed electrode, as shown in Figure 6(a). The SPCE exhibited an electrolytic oxidation signal of 10 m*M* H_2O_2 at +1.4 V with a current response of ~110 μA. No oxidation peak was observed in a blank PBS buffer under identical experimental conditions. Notably, the PPy/PAN–MWCNT/SPCE exhibited a higher anodic current response (420 μA) at a lower potential (+1.2 V). This result is due to the more efficient mass transport and electron transfer properties of the PPy/PAN–MWCNT/SPCE[24]; the conductive nanofiber-covered electrode surface can improve the oxidation reaction area between the electrode surface and H_2O_2. Similarly, the enhancing PPy layer on the conductive nanofibers promotes electron transfer. Such high current values have been previously observed when a PPy layer was incorporated only a screen-printed electrode.[25]

The anodic current of the PPy/PAN–MWCNT/SPCE for H_2O_2 was used to determine whether the electrode could be used as

Applied Polymer SCIENCE

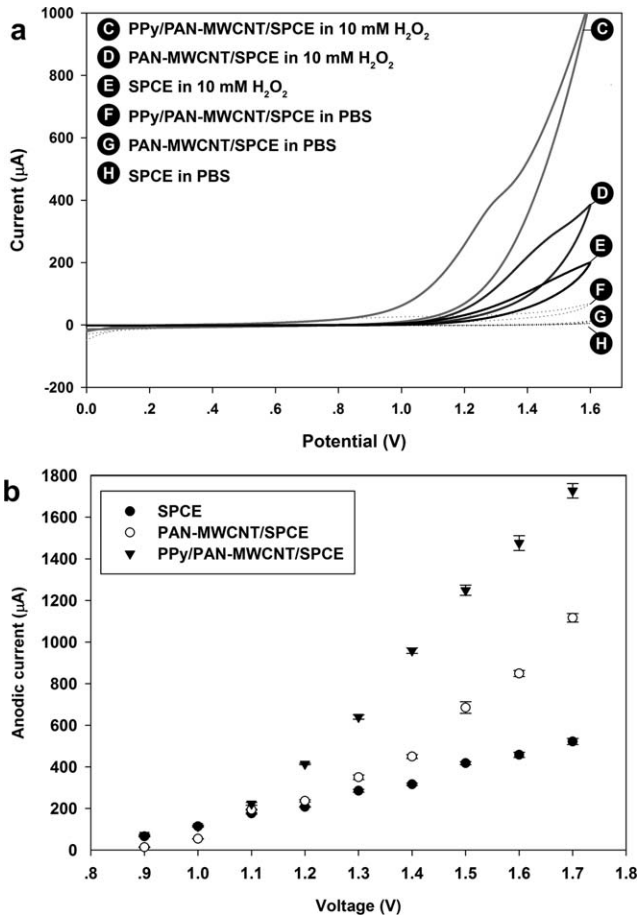

Figure 6. (a) Cyclic voltammograms of the electrodes using 10 m*M* H_2O_2 in 0.1 *M* PBS with a pH of 7.4 at 50 mV/s. (b) Amperometric response of the electrodes using 10 m*M* H_2O_2 in 0.1 *M* PBS with a pH of 7.4 at a fixed potential of +1.4 V for the SPCE and the PAN–MWCNT/SPCE and of +1.2 V for the PPy/PAN– MWCNT/SPCE.

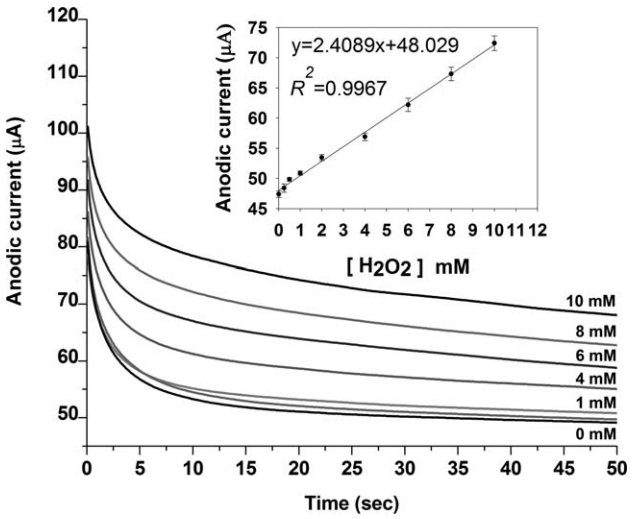

Figure 7. Amperometric responses of the PPy/PAN–MWCNT/SPCE to a sequential increase of glucose in 0.1 *M* PBS with a pH of 7.4; (inset) the linear current response as the H_2O_2 concentration was increased from 0.125 to 10 m*M* at a fixed potential of +1.2 V.

an H_2O_2 biosensor at an applied potential of +1.2 V. Figure 6(b) illustrates the drastically different current responses of the SPCE and the PAN–MWCNT/SPCE, which were fixed at +1.4 V, and the PPy/PAN–MWCNT/SPCE, which was fixed at +1.2 V (i.e., the lowest potential at which H_2O_2 was detected). However, during the amperometric measurement, bubbles were observed to cover the electrode surface when the applied potential was greater than +1.4 V. In addition, the use of an excessively high potential can increase the background current and possibly result in direct oxidation of the electroactive species at the underlying electrode.[31]

The intensity of the signal was shown to be proportional to the H_2O_2 concentration over the studied potential range, as illustrated in the inset in Figure 7. The oxidation peak current varied linearly with concentration in the range from 0.125 to 10 m*M*. The regression equation is given by $y = 2.4089x + 48.029$ ($r^2 = 0.997$), where y and x are the magnitude of the peak current (μA) and the H_2O_2 concentration (m*M*), respectively. The slope of the equation corresponds to a linear sensitivity of 4.77 mA/Mcm^2 and to an LOD of 1.25 μM.

Effect of pH and Buffer Strength on the Anodic Current Response for Hydrogen Peroxide

The effect of pH on the anodic current response of 10 m*M* H_2O_2 detection under various system conditions was also studied. Table I shows that the maximum current response occurred at pH 8. However, at pH 9, the experiment could not be conducted due to bubble formation on the electrode surface (overoxidation). The focus of this study is H_2O_2 detection in a buffer

Table I. The Anodic Current Responses Obtained Using the Amperometric Technique in a 10 m*M* H_2O_2 Solution at Different Ionic Strengths

Anodic current I_p (μA)	pH (0.1 *M* PBS)					Ionic strength of phosphate buffer (*M*), pH 7.4		
	3	5	7.4	8	9	0.050	0.010	0.005
	99.0	232.0	432.2	566.3	n/a	182.7	87.4	65.2
	108.4	244.1	437.9	545.4	n/a	196.5	85.2	64.2
	115.3	243.2	447.0	512.6	n/a	195.7	89.8	67.6
Mean	107.5	239.7	439.0	541.4	-	191.6	87.5	65.6
S.D.	8.1	6.7	7.5	27.0	-	7.7	2.3	1.74

The n/a corresponds to the formation of bubbles on electrode surface.

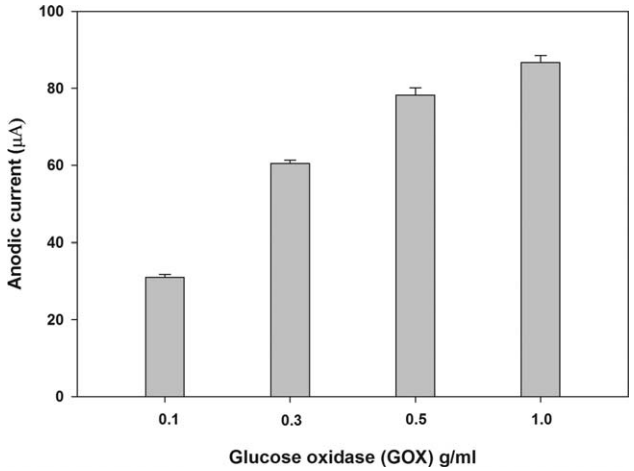

Figure 8. Amperometric peak current of 1 m*M* glucose in various GOX concentrations.

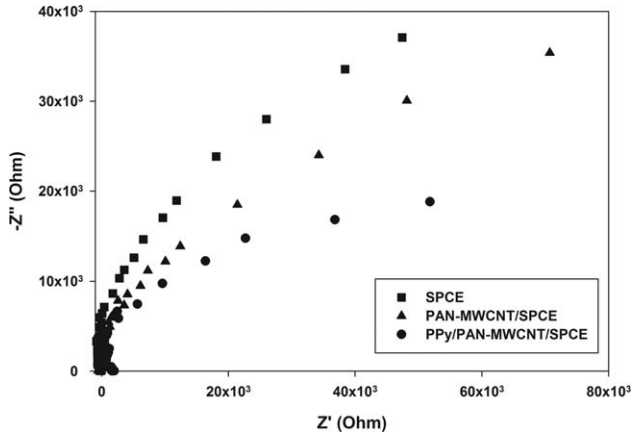

Figure 10. Electrochemical impedance spectroscopy of modified/unmodified electrodes in 5 m*M* of $Fe(CN)_6^{3-/4-}$ solution.

solution, which is commonly used in biological research. Therefore, in further studies, we took measurements at pH 7.4.

Biosensor for Glucose Detection

To study the performance of the H_2O_2 biosensor, which can be used to detect numerous oxidase-substrate compounds based on the catalytic reaction of various enzymes, GOX was chosen as a model enzyme to detect glucose with/without using of a mediator. The amperometric current detection during oxidation at the enzyme electrode follows eq. (2), and the anodic current response at the working electrode follows eq. (3):

$$\beta\text{-D-Glucose} + O_2 + H_2O \xrightarrow{(GOX)} \text{gluconic acid} + H_2O_2 \quad (2)$$

$$H_2O_2 \rightarrow O_2 + 2H^+ + 2e^- \quad (3)$$

In the catalytic reaction between GOX and the glucose molecule, the GOX concentration must be sufficiently high to result in good sensitivity. Figure 8 shows that the anodic current was directly proportional to the GOX concentration up to 1.0 g/mL. The anodic current for GOX concentrations greater than 1.0 g/mL could not be measured due to the low solubility of GOX in the PBS solution. A GOX concentration of 0.1 g/mL was used for both sensitivity and calibration curve, as shown in Figure 9. The amperometric response of the PPy/PAN–MWCNT/SPCE shows that an obvious increase in the oxidation current occurred on the addition of glucose, which was monitored for 50 seconds. The amperometric responses exhibited a linear relation with glucose concentration from 0.25 m*M* to 6.00 m*M* with a correlation coefficient of 0.996 (the inset in Figure 9). The LOD was evaluated to be 15.51 μM, and the sensitivity was 5.41 μA/m*M* cm^2.

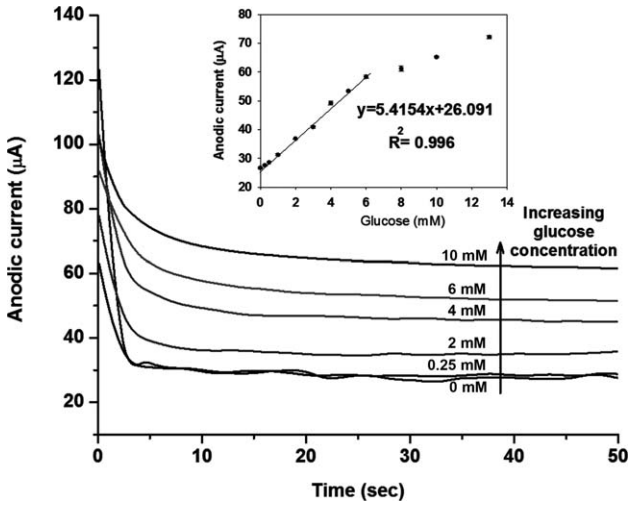

Figure 9. Amperometric measurements obtained for standard glucose additions using an applied potential of +1.25 V for the PPy/PAN-MWCNT/SPCE electrode. The inset is the calibration curve of the PPy/PAN-MWCNT/SPCE electrode.

The problems of using GOX alone in reaction system are the interfere substances, such as ascorbic acid and urea, which can be oxidized at the >0.6 V.[32] So, the anodic current of these compounds could lead to electrochemical interference. The way to eliminate the interference signal is using a mediator. In this study, we used 5 m*M* $Fe(CN)_6^{3-}$ as mediator that can react with GOX instead of oxygen and thus reduced mediator is formed instead of hydrogen peroxide. Equations (4) and (5) show the electron transfer between the mediator and the 0.1 g/mL of GOX in the system reaction. The characteristic of CV PPy/PAN-MWCNT/SPCE was shown in Figure 11. The oxidation peak occurred at +0.36 V with an increase of anodic current toward increasing glucose concentrations.

$$\beta\text{-D-glucose} + 2Fe(CN)_6^{3-} + H_2O \xrightarrow{(GOX)} \text{gluconic acid} + 2H^+ + 2Fe(CN)_6^{4-} \quad (4)$$

$$2Fe(CN)_6^{4-} \rightarrow 2Fe(CN)_6^{3-} + 2e^- \quad (5)$$

The corresponding calibration curve of Mediator+GOX/PPy/PAN-MWCNT/SPCE was evaluated by amperometric technique shown (inset) in Figure 11. Further with this method, glucose can be estimated up to 7 m*M*. Linear current response with concentrations reveal that the Mediator+GOX/PPy/PAN-MWCNT/SPCE can be used to estimate glucose at the low potential with glucose concentration from 0.125 m*M* to 7 m*M* range with LOD (3S/N) of 0.98 m*M* and the sensitivity of this electrode is 14.62 μA/m*M* cm^2

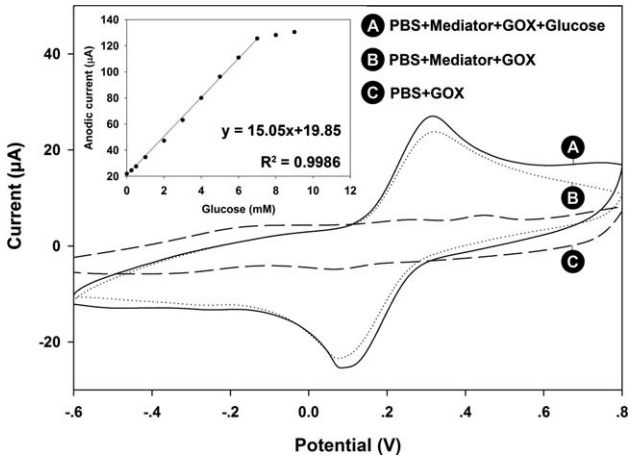

Figure 11. Cyclic voltammograms of the PPy/PAN–MWCNT/SPCE incorporation with mediator for glucose detection in 0.1 *M* PBS with a pH of 7.4; (inset) the linear current response as the glucose concentration was increased from 0.125 to 10 m*M* at a fixed potential of +0.36 V.

The modified electrode exhibited a high sensitivity and a low detection limit because of the high conductivity of the PPy layer and because of the high surface-to-volume ratio of the conductive electrospun fibers that covered the electrode surface. Compared with another report on an amperometric glucose biosensor with a mediator, the LOD in this work was lower than conventional blood glucometers; the detection level was as low as 1.7 m*M*.[11] Moreover, this work has the higher sensitivity than the modification of SPCE surface by using water-based carbon ink containing cobalt phthalocyanine and GOX for the fabrication of a glucose biosensor.[33]

CONCLUSIONS

We have shown that a PPy/PAN–MWCNT/SPCE can be fabricated using electrospinning and VPP techniques. The presence of a conductive nanofiber structure coated with a PPy layer on the SPCE surface enhances the electrochemical redox activity, where the resulting current is produced by radial diffusion and is quasi-reversible with an excellent anodic/cathodic current response and a low ΔE_p in a $Fe(CN)_6^{3-/4-}$ redox-couple system. In the case of standard H_2O_2 detection, the PPy/PAN–MWCNT/SPCE gave a well-defined electrocatalytic response, which indicated that the modified electrodes behave as a disposable device with an anodic current greater than that of the conventional planar SPCE and could be used to measure H_2O_2 over a wide concentration range from 0.125 to 10 m*M*. The incorporation of GOX as an enzymatic model with/without mediator the PPy/PAN–MWCNT/SPCE led to glucose detection over a linear range of 0.125–7 m*M* at +0.36 V and 0.25–6 m*M* at +1.25 V, respectively. This work represents our first report on SPCE surface modification. In future works, enzymatic immobilization on a PPy layer will be investigated.

ACKNOWLEDGMENTS

This work was supported in part by the Chulalongkorn University Dutsadi Phiphat Scholarship, the National Nanotechnology Center (NANOTEC) research fund (RES_54_198_63_006), and the Electrochemistry and Optical Spectroscopy Research Unit, Faculty of Science, Chulalongkorn University, Thailand.

REFERENCES

1. Soo, M. T.; Cheong, K. Y.; Noor, A. F. M. *Sens. Act. B: Chem.* **2010**, *151*, 39.
2. Rawsona, F. J.; Purcellb, W. M.; Xuc, J.; Pembertona, R. M.; Fieldend, P. R.; Biddlee, N.; Harta, J. P. *Talanta* **2009**, *77*, 1149.
3. Thanyani, S. T.; Roberts, V.; Siko, D. G. R.; Vrey, P.; Verschoor, J. A. *J. Immunol. Meth.* **2008**, *332*, 61.
4. Zheng, S.; Zhu, Y.; Krishnaswamy, S. *Sens. Act. B: Chem.* **2013**, *176*, 264.
5. Yanga, R.; Huangb, X.; Wanga, Z.; Zhoua, Y.; Liu, L. *Sens. Act. B: Chem.* **2010**, *145*, 474.
6. Wu, J.; Yin, L.; *ACS Appl. Mater. Interfaces* **2011**, *3*, 4354.
7. Chang, H.; Yuan, Y.; Shi, N., et al. *Anal. Chem.* **2007**, *79*, 5111.
8. Donavan, K. C.; Arter, J. A.; Pilolli , R.; Cioffi, N.; Weiss, G. A.; Penner, R. M. *Anal. Chem.* **2011**, *83*, 2420.
9. Ahmad, M.; Pan, C.; Luo, Z.; Zhu, J. *J. Phys. Chem. C* **2010**, *114*, 9308.
10. Kiran, R.; Scorsone, E.; Mailley, P.; Bergonzo, P. *Anal. Chem.* **2012**, *84*, 10207.
11. Dungchai, W.; Chailapakul, O.; Henry, C. S. *Anal. Chem.* **2009**, *81*, 5821.
12. Liu, Y.; Feng, X.; Shen, J., et al. *J. Phys. Chem. B* **2008**, *112*, 9237.
13. Karuwan, C.; Sriprachuabwong, C.; Wisitsoraat, A.; Phokharatkul, D.; Sritongkham, P.; Tuantranont, A. *Sens. Actuators B: Chem* **2012**, *161*, 549.
14. Ju, Y.-W.; Choi, G.-R.; Jung, H.-R.; Lee, W.-J. *Electrochim. Acta* **2008**, *53*, 5796.
15. Choi, J.; Park, J. E.; Park, W. D.; Shim, E. S. *Synth. Met.* **2010**, *160*, 2664.
16. Jang, K.-S.; Eom, Y.-S.; Lee, T.-W.; Kim, D. O.; Oh, Y.-S.; Jung, H.-C.; Nam, J.-D. *ACS Appl. Mater. Interfaces* **2009**, *1*, 1567.
17. Laforgue, A.; Robitaille, L. *Macromolecules* **2010**, *43*, 4194.
18. Subramaniana, P.; Clarkb, N. B.; Spicciaa, L.; MacFarlanea, D. R.; Winther-Jensenc, B.; Forsytha, C. *Synth. Met.* **2008**, 158, 704.
19. Kim, J.-Y.; Lee, J.-H.; Kwon, S.-J., *Synth. Met.* **2007**, *157*, 336.
20. Chae, H. G.; Sreekumar, T. V.; Uchida, T.; Kumar, S. *Polymer* **2005**, *46*, 10925.
21. Laforgue, A.; Robitaille, L. *Chem. Mater.* **2010**, *22*, 2474.
22. Njagi, J.; Andreescu, S. *Biosens. Bioelect.* **2007**, *23*, 168.
23. Palomeraa, N.; Verac, J. L.; Meléndezc, E.; Ramirez-Vickb, J. E.; Tomard, M. S.; Aryae, S. K.; Singhb, S. P. *J. Electroanal. Chem.* **2011**, *658*, 33.

24. Chronakis, I. S.; Grapenson, S.; Jakob, A. *Polymer* **2006**, *47*, 1597.

25. Ji, L.; Yao, Y.; Toprakci, O.; Lin, Z.; Liang, Y.; Shi, Q.; Medford, A. J.; Millns, C. R.; Zhang, X. *J. Power Sources* **2010**, *195*, 2050.

26. Lakarda, B.; Seguta, O.; Lakarda, S.; Herlema, G.; Gharbib, T. *Sens. Actuators B: Chem.* **2007**, *122*, 101.

27. Atta, N. F.; Galal, A.; Khalifa, F. *Appl. Surf. Sci.* **2007**, *253*, 4273.

28. Frasconi, M.; Favero, G.; Di Fusco, M.; Mazzei, F. *Biosens Bioelect* **2009**, *24*, 1424.

29. Bonastrea, J.; Garcésb, P.; Galvánc, J. C.; Casesa, F. *Prog. Org. Coat.* **2009**, *66*, 235.

30. Iroh, J. O.; Levine, K., *J. Power Sources* **2003**, *117*, 267.

31. Gao, Z.; Xie, F.; Shariff, M.; Arshad, M.; Ying, J. Y. *Sens. Actuators B: Chem* **2005**, *111–112*, 339.

32. Lee, S. R.; Lee, Y. T.; Sawada, K.; Takao, H.; Ishida, M. *Biosens. Bioelectron.* **2008**, *24*, 410.

33. Crouch, E.; Cowell, D. C.; Hoskins, S.; Pittson, R. W.; Hart, J. P. *Anal. Biochem.* **2005**, *347*, 17.